UNIVERSITATEA "BABEŞ-BOLYAI" CLUJ-NAPOCA

FACULTATEA DE FIZICĂ

BIOFIZICĂ ŞI FIZICĂ MEDICALĂ

LUCRARE DE DISERTAŢIE

Coordonatori ştiinţifici

Prof. Vasile CHIŞ, PhD

Prof. Olivier CHAPET, MD, PhD

Corina UDRESCU, MD, PhD

Université Claude Bernard Lyon 1, Hôpital Lyon Sud

Absolvent

Elena NEDELCU

2025

UNIVERSITATEA “BABEŞ-BOLYAI” CLUJ-NAPOCA
FACULTATEA DE FIZICĂ
BIOFIZICĂ ŞI FIZICĂ MEDICALĂ

LUCRARE DE DISERTAŢIE

MIŞCAREA INTERFRACŢIONALĂ A UTERULUI ÎN TIMPUL RADIOTERAPIEI LA PACIENTELE TRATATE PENTRU CANCER DE COL UTERIN CU UNITY® MR-LINAC

INTER-FRACTION MOTION OF UTERUS DURING RADIOTHERAPY IN PATIENTS TREATED FOR CERVICAL CANCER AT UNITY® MR-LINAC

Coordonatori ştiinţifici

Prof. Vasile CHIŞ, PhD

Prof. Olivier CHAPET, MD, PhD

Corina UDRESCU, MD, PhD

Université Claude Bernard Lyon 1, Hôpital Lyon Sud

Absolvent

Elena NEDELCU

2025

Abstract

Cervical cancer, with serious rates of mortality and morbidity, poses difficulties in therapeutic strategies on account of the inherent pelvic organ dynamics. As an integral part of treatment approaches, radiotherapy presents impressive precision capabilities with the aid of MR-guided adaptive systems, being improved by potential predictable motions. An example that highlights the significance of this aspect is the uterine movement.

Thus, this paper aimed to evaluate interfraction motion of uterus during radiotherapy delivered with Elekta Unity ® MR-Linac, in relation with uterine flexion characteristics. The cohort comprising of nine patients was assessed by using daily MRI scans corresponding to 25 fractions and by firstly registering the DICOM coordinates for four essential anatomical points – superior and inferior pubic symphysis, coccyx and tip of the external uterus fundus position on the axis of endometrium – that spatially form a pyramid. The analysis included reconstructing the geometrical structures on the first fraction anatomy. Moreover, the superior-inferior deviation was described by an angle in the sagittal plane, chosen relative to a vertical axis. Data processing and interpretation consisted of directional vectors to describe the general displacement, ellipsoid modelling to define motion features and statistical significance analysis.

The results revealed a relevant statistical general response to the bladder filling of the normal and anteverted uteri, with a tendency towards the anterior-posterior and superior-inferior directions, in contrast to the retroverted uteri that exhibited reduced or absent correlations. The predominant directional movement was highlighted by the vertical-oriented angle deviation that positively responded to the bladder volume changes in the case of normal and anteverted configurations.

This study firmly supports the importance of bladder filling management protocols and personalized uterine margins in order to reach the potential of MR-guided adaptive techniques, further contributing to important advancements in radiotherapy strategies.

List of Abbreviations

AP – anteroposterior direction

ART – adaptative radiotherapy

ATP – adapt-to-position

ATS – adapt-to-shape

CC – craniocaudal direction

CT – computed tomography

DICOM - digital imaging and communications in medicine

DSC – dice similarity coefficient

EBRT – external beam radiotherapy

FIGO - International Federation of Gynecology and Obstetrics

HPV - human papillomavirus

IGRT – image-guided radiotherapy

IMRT – intensity modulated radiotherapy

LEEP - loop electrosurgical excision procedure

LR – left-right direction

MRgRT – magnetic resonance-guided radiotherapy

MRI – magnetic resonance imaging

OAR – organ-at-risk

SCC - squamous cell carcinoma

SIB – simultaneous integrated boost

VIA - visual inspection with acetic acid

VMAT – volumetric modulated arc therapy

List of Figures

List of Tables

Contents

Introduction

Cervical cancer is globally categorized among the most prevalent and deadly, calling for strategies in order to mitigate the incidence and to eventually eliminate the risks [1, 2]. Beside the need of vaccination for human papillomavirus (HPV) as a prevention measure and screening programs that contribute to early detection, the treatment approaches require constant advancements [3, 4]. To this end, radiotherapy, an integral part of cervical cancer management, involves various aspects that need to be considered in order to achieve complete effectiveness, notably including organ motion and accurate target repositioning [5, 6].

This study was conducted to assess the interfractional uterine movement and flexibility in connection with bladder in cervical cancer cases treated with Elekta Unity® MR-Linac. Consequently, including ten patients, the analysis was conducted on 250 MRIs and involved distances and angle measurements carried out by the means of a specialized software.

The thesis is comprised of three major chapters that intend to focus on reaching a conclusion in relation to the aforementioned topic. The first chapter aims to create an overview of cervical cancer, the anatomical aspects of the cervix and uterus, their implications and treatment methods, with an emphasis on adaptive radiotherapy and its usefulness in understanding the pelvic organs evolution throughout the therapeutical period. The second chapter consists of details regarding the methodology that could be summed up to the patient's characteristics, treatment planning aspects, the organ delineation, the steps concerning the distance and angle measurements performed to determine the uterine motion and analysis. The resulted data are compressed in the third chapter that intend to reach a general conclusion regarding the interfraction movement based on the uterus configuration, during radiotherapy in patients treated for cervix cancer at Unity® MR-Linac. Moreover, this chapter's relevance lies in the inclusion of the interpretation of the results, the statistical study and the comprehensive analysis. The concluding section encapsulates the principal inferences drawn from the present research, while concurrently describing its inherent methodological and theoretical limitations. Furthermore, it describes the potential for continued advancement within this field of research.

1. Fundamental notions of cervical cancer

With around 660 000 new cases and 350 000 deaths globally in 2022, cervical cancer is ranked fourth in both incidence and mortality rates among women, according to Global Cancer Observatory [1, 2]. The Cervical Cancer Elimination Initiative was adopted in 2020 by the World Health Organization as a global strategy that envisions an incidence reduction to fewer than 4 cases per 100,000 women in every country [3, 4]. At its core, the plan revolves around three fundamental components: prevention with widespread vaccination efforts, early detection determined by robust screening programs, and comprehensive cancer management and treatment.

1.1. Cervix and uterus anatomy

Situated between the bladder and rectum, the uterus, a central component of the female reproductive system, is a muscular organ that is anatomically divided in: the fundus, the superior portion linked to the fallopian tubes, the corpus uteri that is the principal section, the isthmus and cervix [7]. The cervix is the fibrous and muscular pelvic organ that is connected to the corpus via the isthmus [8]. It typically measures about 4 cm long and 3 cm wide, serving as the connection between the uterus and the vagina [9]. The cervix is superiorly limited by the internal os, while the inferior part that opens to the vagina is the external os. The portion of the cervix lying exterior to the external os is called the ectocervix, lined with squamous epithelium, and meets the endocervix that forms the endocervical canal, with glandular epithelium, at the squamocolumnar junction, aspects that are represented in Figure 1.1 [9 - 10]. The cervix, as part of the uterus, plays key roles in pregnancy, menstruation and childbirth [7].

1.2. Cervical cancer

There are mainly two types of cervical cancer that are individualised based on the anatomical emergence site: *squamous cell carcinoma (SCC)*, specific for ectocervix and the most prevalent, and *adenocarcinoma*, developed in the endocervix [10]. While many women remain symptom-free, possible symptoms include postcoital bleeding, intermenstrual bleeding, excessive vaginal discharge, and pain in the pelvic region or lower back area [11]. The three key tests used for cervical cancer screening include cytology (PAP Smear), HPV testing, and visual inspection with acetic acid (VIA). Ongoing untreated HPV infection accounts for 99.7% of cervical cancer cases

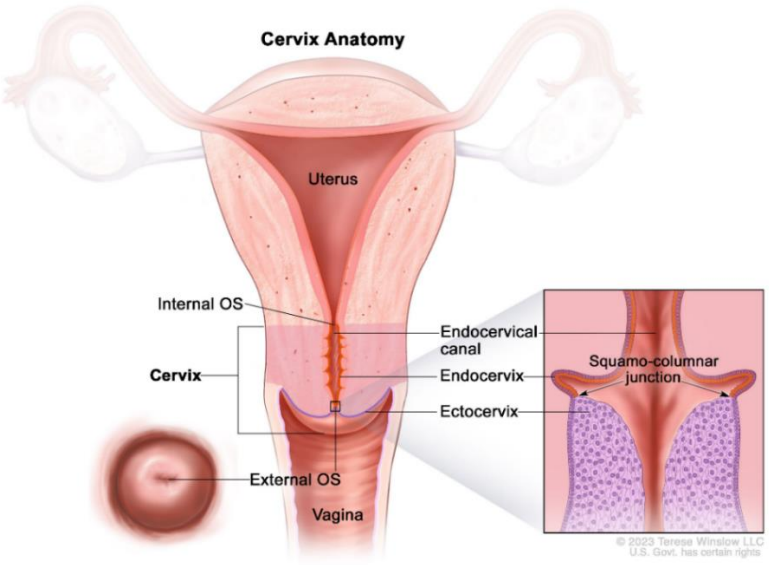

Figure 1.1: Cervix anatomy [10]

[12]. The diagnostic process is generally initiated following *an abnormal* screening result that requires further investigations such as colposcopy or biopsy [13]. In case of confirmed presence of cancer, to ensure a suitable clinical course of action, the next step is to thoroughly assess disease severity and extent using imaging techniques, lab examinations or visual tests [14]. This necessity led to a compilation and classification made by the International Federation of Gynaecology and Obstetrics (FIGO) that considered the *tumour size, its location and spread degree* to *create* a staging system under continuous revision and improvement [15 - 17].

1.3. Treatment strategies for cervical cancer

In terms of treatment, depending primarily on the stage, cervical cancer commonly requires comprehensive approaches that range from surgical procedures to external beam radiotherapy (EBRT) concurrently delivered with chemotherapy, typically cisplatin at 40 mg/m² weekly, and completed by subsequent brachytherapy for locally advanced cervical cancer [18 - 21].

Surgery is widely employed in order to remove the affected tissue in case of early-stage cervical cancer and includes interventions such as conization, total and radical hysterectomy, trachelectomy, cryosurgery or loop electrosurgical excision procedure (LEEP) [12, 22].

1.4. Radiotherapy

The EBRT, as an integral part of the standard treatment strategy, consists of administering 45 to 50 Gy in 25 fractions to the target volumes defined during the first steps of treatment planning [5]. However, there are various sources of uncertainty that render it infeasible to replicate the planning configuration with complete accuracy during the treatment period, among which the inner organs' displacements are the most relevant.

Due to the inherent tendency of pelvic organs to shift in position and volume, the correlation between planning and treatment processes is influenced/affected by inconsistencies in anatomical structures [6, 23, 24]. As bladder and rectum fill, owing to characteristic high mobility, movement of tumour and adjacent organs, such as uterus, occurs, thereby leading to increased predisposition to underdosage of the cervix target volume or/and to excessive exposure of the organs-at-risk (OAR) or healthy tissues in case of radiotherapy [21, 24 - 30]. Additionally, as the tumour shrinks in response to treatment, it greatly impacts the position of surrounding anatomical structures, highlighting the requirement for significant margin adjustments [25, 30]. The extent of motion is inherently patient-specific, and its anticipation enables the tailoring of treatment approaches to individual anatomical and physiological characteristics, hence minimizing unnecessary dose exposure to adjacent OARs.

Recently, the implementation of modern EBRT techniques such as intensity modulated radiation therapy (IMRT) and volumetric modulated arc therapy (VMAT), have enhanced the conformity of the dose distribution to the target [31, 32]. Consequently, reductions in the overall irradiated volumes have led to improved sparing of OARs; however, this has concurrently increased the risk of target under-dosage in patients experiencing considerable anatomical motion [32]. To this end, accurate anticipation/prediction of inter-fractional target position variability becomes essential for each individual patient.

1.4.1. Imaging of the cervix

These aspects pose great difficulty in achieving the radiotherapeutic goals in the absence of the image-guided (IGRT) technologies, such as cone-beam CT (CBCT), to account for the complexity of pelvic anatomy and for the set-up and patient positioning errors [33].

Furthermore, with respect to the significant impact of diagnostic and treatment advancements, the latest update of FIGO also emphasises the enhanced role of magnetic-resonance imaging (MRI) in precise tumour evaluation and disease extent, by virtue of its superior soft-tissue discrimination capabilities in absence of radiation exposure in opposition to computed tomography (CT) [15 - 18, 25, 34 - 38]**.** Additionally, MRI provides outstanding reliability in early detection of residual tumour following radiation therapy and in identifying disease recurrence during follow-up evaluations [39].

1.4.2. MR-guided radiotherapy – Adaptative radiotherapy

Moreover, the significant organ intra- and inter-fraction flexibility and the immense variability between patients, to which the MRI advantages are added, introduced the online MR-guided radiotherapy (MRgRT) as a valuable adaptive radiotherapy (ART) solution [25]. ART is characterized by real-time adjustments to the treatment plan in response to anatomical changes such as weight variations, tumor shrinkage, or internal organ movement throughout the course of therapy [40 - 43]. Studies revealed the superiority of MRgRT in image quality and in minimizing observer-related variability during contour delineation, in contrast to its undeniable technical challenges and difficulties in being implemented [25, 42]. In cervical cancer treatment, ART offers the means to improve the precision by accounting for inter-fraction motion of the bladder, rectum and uterus, that significantly decreases the toxicity, through smaller margins, enhanced treatment accuracy and target localization [25, 44, 45]. These advancements also stem from the creation of the MRI-Linac which merges MRI technology with a linear accelerator to support adaptive workflows.

Figure 1.2: Elekta Unity® [46]

1.4.3. MRI-Linac - Elekta Unity®

Elekta Unity®, one of the commercially available MR-guided radiotherapy systems, was introduced in 2018 and is produced by Elekta AB (Stockholm, Sweden) [47 - 49]. It features advanced technology that integrates a Philips-manufactured 1.5T MR and a 7MV linear accelerator designed by Elekta, presented in Figure 1.2. The system operates in conjunction with Elekta MOSAIQ® and Elekta Monaco®, a treatment planning system employing Monte Carlo simulations designed to enable precise dose distribution optimization and calculation within a magnetic field environment [50]. Depending on the daily clinical evaluation, there are two workflows that can be chosen: adapt-to-position (ATP) or adapt-to-shape (ATS) [51]**.** While the ATP workflow addresses minor positional changes by only shifting a virtual isocenter on the online MRI relative to the simulation CT, the ATS workflow poses more challenges as it focuses on tumours and OARs with daily deformations that require recontouring and replanning, ideas schematized in Figure 1.3 [51 - 54]**.** Thus, the system effectively addresses the comprehensive requirements of real-time delivery control and inter-fractional motion management, yielding a substantial enhancement on the treatment outcome [55].

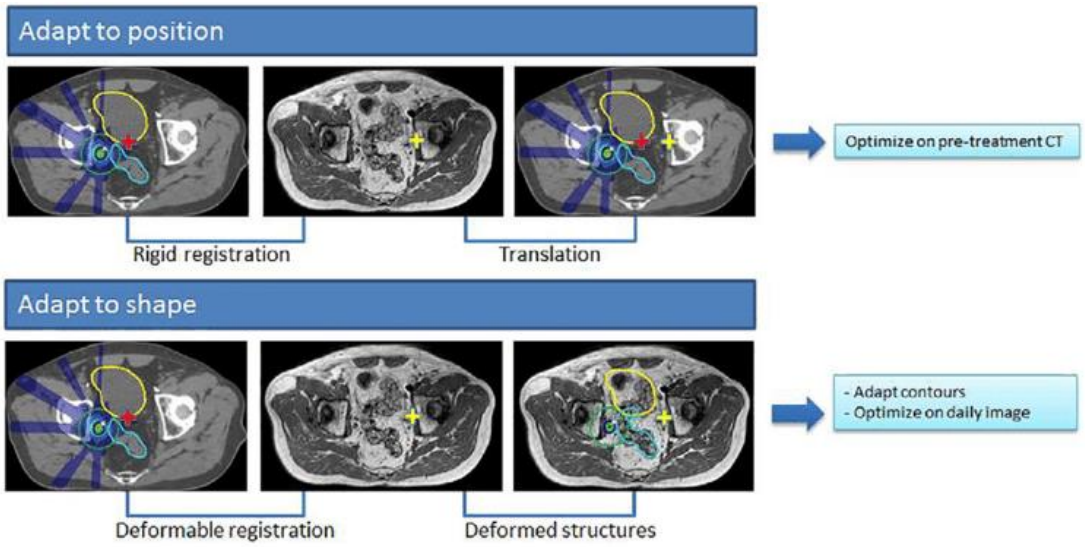

Figure 1.3: Overview of the adapt-to-position and adapt-to-shape workflows in the case of lymph node oligometastases [53].

1.5. Literature review – Inter-fraction motions in cervical cancer overview

Previous analyses have been conducted to provide insights into the intra- and inter- fraction pelvic organ motions and tumour evolution, using MRI systems in case of cervical cancer [6, 29, 56]. In a previous study, by employing weekly 30-minutes cinematic-MRI (GE Signa Excite 1.5T), Chan *et al.* measured interscan and intrascan motions of specific anatomical points of cervix-uterus structure and evaluated the correlation with bladder and rectal filling [56]. The mean interscan displacements in craniocaudal (CC) and anteroposterior (AP) directions, ranged from 5.7 to 24.4 mm and from 4.8 to 14.5 mm, with a 40 mm motion of uterine fundus and with intrascan movements being considerably less evident. Furthermore, Taylor *et al.* focused on investigating the movement of the uterus and cervix between fractions to identify suitable internal margins in the context of gynaecological cancer, including cervical cancer [29]. Using MRI scans on two successive days, the displacement analysis of three relevant points provided mean values in the ranges of 2.6 - 7.0, 2.7 - 7.1 and 0.3 - 0.8 mm in the AP, CC and lateral (LR) directions. While bladder filling was linked to the change of uterine position in the CC direction, cervical and vaginal AP motions were predominantly impacted by the rectal filling. In addition, a comprehensive summary of studies examining pelvic organ intrafraction movement is provided in the Jadon *et al.* systematic review, with results for the uterus and cervix in the mean range of 0.1 - 3.0 mm and no significant directional trend observed [6].

1.5.1. Studies using an MRI-Linac

Recent studies focused on the significant capabilities of the MRgRT technology to build upon these findings, employing refined statistical and scientific methods to yield an enhanced outlook on/ provide an enhanced understanding of the pelvic organ variations in the context of cervical cancer. Nagao *et al.* primarily addressed the intrafractional cervix-uterus motion and its impact on the adjacent organs, namely the bladder and rectum volumes [57]. The displacement was evaluated using the dice similarity coefficient (DSC), which quantifies the coincidence between two contours. Thus, in the cases where bladder or rectum volume changes correlated with uterus or cervix DSC, increased volume variations led to reduced DSCs, indicating a pronounced shift in uterine or cervical position. Another significant conclusion was that bladder filling generally causes an uterine displacement in the superior and posterior directions [57]. Li *et al.* used various measurement techniques with the aim of evaluating the intra- and inter-fraction changes in position of uterus as well as in bladder volume

[58]. A notable correlation between the bladder volume variation and the cervix-uterus movement was identified as daily MRI scans, before and after each fraction, were used to measure the organ motions. The cervical-uterine intra- and inter-fractional displacement averaged to 11.5 and 10.3 mm in CC direction and to 6.11 and 5.9 mm in AP direction [58]. Kishigami *et al.* used a shape model and daily MR images acquired with a MRgRT system to independently evaluate the interfractional uterine and cervical motion in three-dimensional space [59]. They concluded that the diminished cervical volume at the 16th fraction supports the need for replanning as the treatment progress inferred tumour softening as well as increased cervix and uterus motion. While cervical population-based margins in (R, L, A, P, S, I) were (7, 7, 11, 6, 11, 8) mm, for the uterus, the results were (14, 13, 27, 19, 15, 21) mm, values established as the 90th percentile values of the patient-specific margins. Moreover, the analysis indicated that the relationship between cervical volume variations and the displacement of both the cervix and uterus yielded weak correlation coefficients [59].

2. Materials and Methods

2.1. Patients

As part of this retrospective study conducted at the Department of Oncology and Radiotherapy of Lyon Sud Hospital, 18 patients with cervical cancer that underwent radiotherapy on Elekta Unity® MR-Linac 1.5T (Elekta AB, Stockholm, Sweden), between July 2021 and December 2023, were included. Chemotherapy with 40 mg/m2 of cisplatin per weekly cure was delivered concomitantly for eight patients.

2.2. Treatment planning

The prescribed dose was 45 Gy in 25 fractions, delivered with intensity modulated radiotherapy (IMRT), that was supplemented with a boost of 55 Gy, with the simultaneous integrated boost (SIB) technique in the case of lymph nodes involvement. The preparatory protocol for each fraction involves urinating one hour prior to the treatment and drinking 500 ml of water, with the aim of a comfortable and repeatable bladder filling. Emptying the rectum was recommended before each fraction as well.

2.3. Organ and tumour delineations

For each patient and at each fraction, using Elekta Monaco®, the bladder, rectum and uterine volumes were precisely delineated by two radiation oncologists on an T2-weighted MRI scan, using Elekta Monaco® treatment planning system. In total, 250 MRI scans were acquired, contoured and validated.

2.4. Measurements

In order to verify the existence of patterns in the uterus shift over the 25 treatment fractions in relation with uterine flexion features (anteverted, normal and retroverted), an analysis based on geometrical aspects was done. For each MRI scan, the distances from the pubic symphysis (D_{ssu}, D_{siu}) and coccyx (D_{cu}) to the external uterine fundus were calculated by registering the DICOM coordinates (x, y, z) of each point and using the Euclidean distance formula (1):

$$D_{ij} = \sqrt{(x_j - x_i)^2 + (y_j - y_i)^2 + (z_j - z_i)^2} \quad (1)$$

The references for the pubic symphysis were determined as the most posterior-inferior (si) and anterior-superior points (ss) in the sagittal slice that included its midpoint in the axial plane. The

reference point for the coccyx (c) was determined by identifying the first axial plane slice in which the bone was clearly visible. Within this slice, the point was selected at the midpoint of the coccygeal bone to ensure consistent anatomical referencing. The measurement point for the external uterine fundus (u) was selected on the sagittal slice where the endometrium was most distinctly visible and was specifically positioned along the axis of the endometrium. A 2D representation of the organ delineation, the reference points and the distances is shown in Figure 2.1.

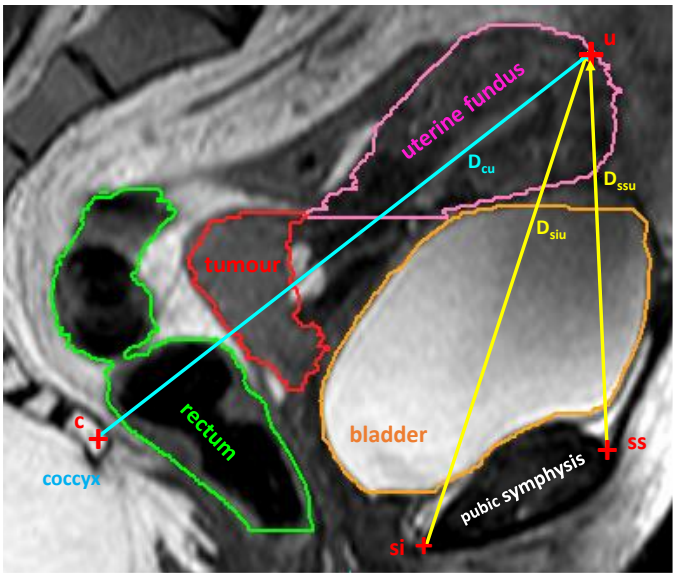

Figure 2.1: Sagittal image of a T2-weighted MRI that shows the delineated volumes (rectum - green, uterus - pink, bladder - orange, tumour - red), the reference points (coccyx - c, pubic symphysis – ss, si, external uterine fundus - u) and the calculated distances (D_{cu} - distance from the coccyx to the uterine fundus, D_{ssu} - distance from the superior symphysis to the uterine fundus, D_{siu} - distance from the superior symphysis to the uterine fundus)

In addition, it was considered that the four points created a pyramidal structure, wherein the apex corresponded to the tip of the uterine fundus, and the base was defined by the triangular plane formed by the pubic symphysis and coccygeal reference points, as presented in Figure 2.2. All the 9 angles, for each of the fractions, were calculated using a Python code that employs the dot product formula (2):

$$\vec{a} \cdot \vec{b} = |\vec{a}||\vec{b}|cos(\alpha) \quad (2)$$

As the reference bony structures have fixed position, the uterus motion over the treatment period was assessed relatively to the first fraction for every patient. Thus, the distances and angles obtained for each fraction were used to systematically build the 24 pyramidal structures with the first fraction reference points as the triangular base. In this way, it was possible to achieve a spatial distribution of uterine movement that was described by an ellipsoid. The centroid was determined by the mean value of the constructed pyramids' coordinates and the axes resulted from the standard deviations along each principal direction. To accurately compute and visualize these geometrical structures and values, a straightforward Python code was employed. The inputs were the DICOM x, y, z coordinates of the4 anatomical points – ss, si, c, u – and 3 angles (β, s_1 and c_1 – see Figure 2.2) corresponding to the initial fraction.

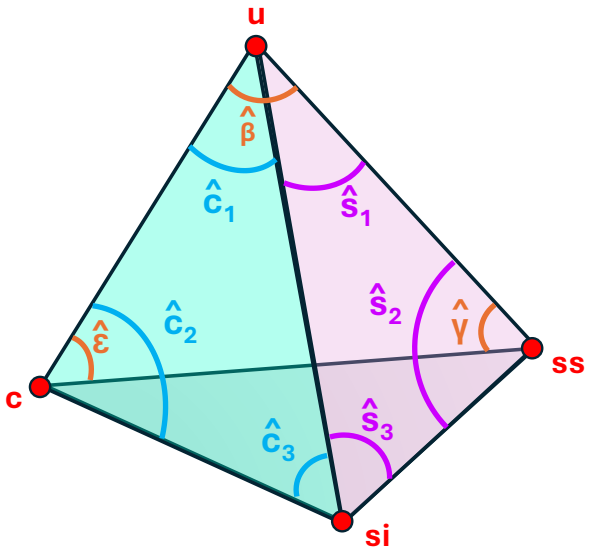

Figure 2.2 – The visual representation of the pyramidal structure formed by the four reference points (ss – superior pubic symphysis, si – inferior pubic symphysis, c – coccyx, u – uterus fundus)

Furthermore, to evaluate the influence of bladder volume on uterine angulation, three specific anatomical reference points were selected for each treatment fraction in order to define a relevant angle. In addition to the previously described point located at the uterine fundus tip, two supplementary points were selected within the same sagittal plane. Thus, the first of these was positioned along a vertical axis parallel to the treatment couch and passing through the zone of the S1-L5 vertebrae, at the most inferior region, known as sacral promontory. The second point was

defined as the intersection between the axis of the endometrium that includes the uterine fundus point and the aforementioned vertical axis. This geometric configuration allowed for the consistent measurement of uterine angulation (α) across treatment sessions (S), as illustrated in Figure 2.3. Additionally, in particular cases - when the intersection point coincides with the uterine tip or the S1-L5 anatomical landmark, when no intersection occurs or when the uterine movement is oriented in the opposite direction - it was necessary to employ alternative strategies. These included selecting different points along the respective axes, utilizing parallel axes or applying geometric formulas to accurately determine the required angle while maintaining its anatomical and functional relevance.

For each of these points, the DICOM coordinates were registered and used in the mentioned Python code that employs the dot product formula (2) in order to calculate the angle (α) formed by the respective lines.

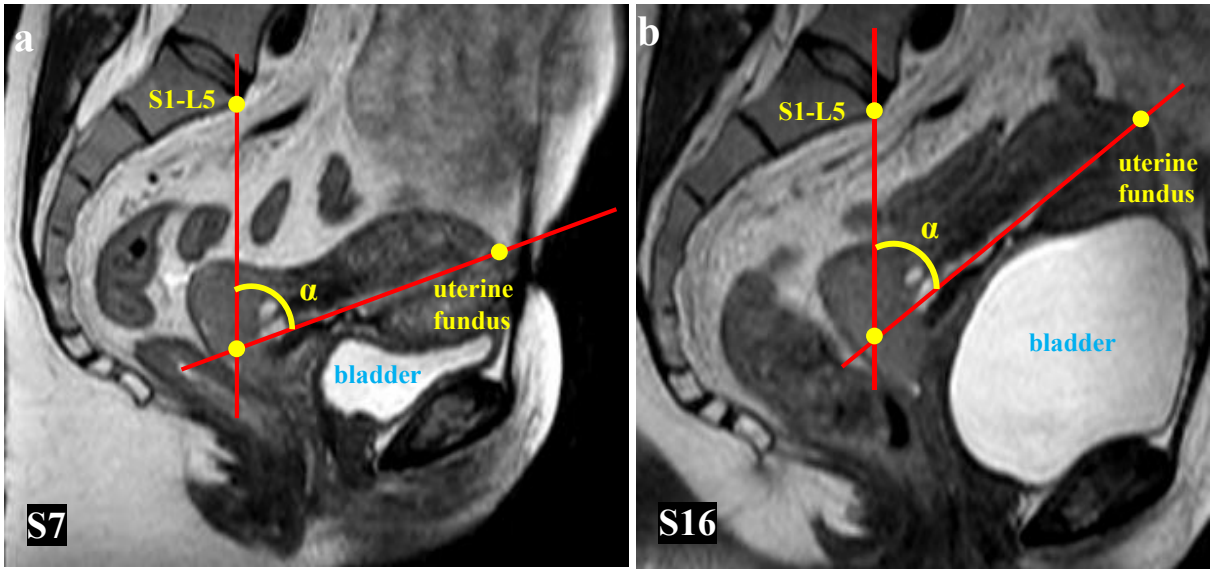

Figure 2.3: Uterine angulation representation for two sagittal MRIs from Patient 2, corresponding to the a) seventh (S7) and b) sixteenth (S16) treatment sessions

2.5. Analysis

The raw data were imported into Microsoft Excel (Microsoft Corporation, Redmond, Washington) for processing. With the aim of revealing meaningful patterns, removing the substantial inter-patient

variability and improving the visualization, the relative change values with respect to the first treatment fraction were calculated.

The Python scripts were run using Visual Code Studio (Microsoft Corporation, Redmond, Washington) editor that, by employing plotting-specialized modules (matplotlib library), also produced the three-dimensional graphs.

To examine the reproducibility of uterine motion across the treatment period, Pearson's correlation coefficient and the significance relevance between its displacement (Δd), based on the obtained coordinates relative to the first fraction (Δx, Δy, Δz), and the corresponding change in bladder volume (ΔV_B) have been evaluated. The same method was used to observe the correlation between the relative change in uterus angle with respect to the vertical axis and relative change in bladder volume. The statistical significance has been evaluated based on p-values, with a threshold of $p < 0.05$ being considered as statistically relevant.

3. Results

3.1. Patients

Eight patients out of 18 were excluded because of incomplete treatment due to psychological reasons, prior treatments involved or only the boost was delivered with this machine. Moreover, after the first step involving the contouring, one more patient (P03) was excluded because of software technical difficulties. The general details concerning the pathology, treatment and characteristics of the other patients (P01 – P10) are included in Table 3.1. The three groups established according to the uterus flexion were evaluated for the following patients: anteverted (A) – P04, P08 P10, retroverted (R) – P01, P06, P09 and normal (N) – P02, P05, P07, as represented in Figure 3.1.

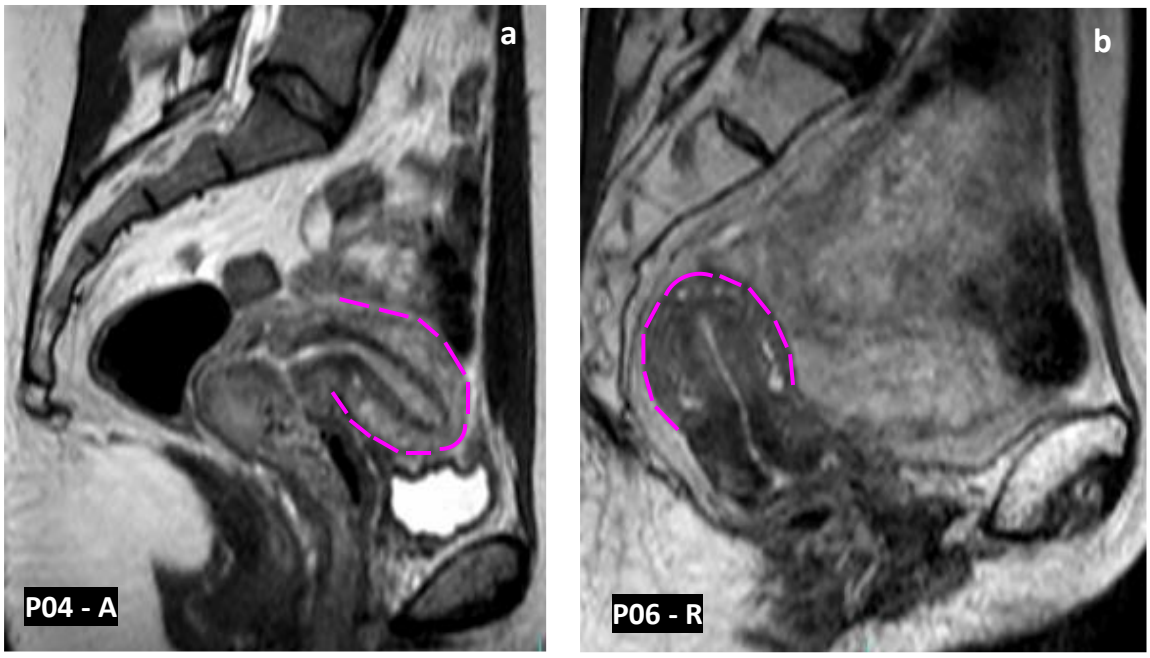

Figure 3.1: Uterine flexion representation for a) P04 that present an anteverted (A) uterus and for b) P06 with a retroverted (R) uterus (outlined in pink colour for more facile distinction)

Table 3.1: Clinicopathologic characteristics of patients

Characteristic	
Age (years)	
Median (range)	52 (26 - 94)
	No. of patients (%)
Histological features	
Squamous cell carcinoma	7 (77.8)
Adenocarcinoma	2 (22.2)
HPV status	
HPV +	8 (88.9)
HPV -	1 (11.1)
FIGO stage	
IB	1 (11.1)
IIA	1 (11.1)
IIB	4 (44.4)
IIIC	3 (33.3)
Uterus flexion	
Anteversion	3 (33.3)
Normal	3 (33.3)
Retroversion	3 (33.3)
Treatment	
IMRT (45Gy / 25 fr.)	6 (66.7)
SIB (55Gy / 25 fr.)	3 (33.3)
Concomitant Chemotherapy	7 (77.8)

3.2. Uterus displacement analysis

The three-dimensional plots in Figure 3.2 – 3.4, resulted after building the geometric structures for each patient based on the anatomy of the first fraction, also produced data about the displacement (Δu) of uterus point (u) and the ellipsoid, found in Table 3.2.

The retroverted uteri display the lowest mean displacement values (0.4 – 1.2 cm), with significant motion in posterior-inferior direction ($\Delta y < 0$, $\Delta z > 0$), ideas that are accentuated by y- and z- axis SD. Then, it is observed that normal uteri present important movement characteristics, with mean values ranging from 1.9 to 4.6 cm and reaching 7.0 cm. The ellipsoidal attributes suggest a predominant tendency of AP and SI displacement. On the other hand, the anteverted uteri regularly shifted in the AP direction (y-axis), with an evident variability in mean displacement values, that amount up to 3.3 cm.

Table 3.2: Displacement data resulted from the three-dimensional plots based on the first fraction anatomical geometry, according to uterus configuration

Uterus	***ID***	***Displacement [cm]***						***Ellipsoid – SDs [cm]***		
		Mean ± SD	***Max***	***Δx***	***Δy***	***Δz***	***Dir.***	***x***	***y***	***z***
R	**P01**	1.2 ± 0.5	2.3	-0.1	-0.8	0.6	AP	0.1	0.8	0.7
	P06	0.9 ± 1.0	4.8	-0.1	-0.5	0.9	SI	0.2	1.1	1.9
	P09	0.4 ± 0.3	0.9	0.0	-0.6	0.8	SI	0.0	0.4	0.6
N	**P02**	3.6 ± 1.5	5.3	0.0	-1.0	0.0	AP	0.0	2.9	0.1
	P05	4.6 ± 1.0	7.0	-0.1	-0.6	0.8	SI	0.1	1.2	1.7
	P07	1.9 ± 1.3	4.3	0.0	0.9	-0.4	AP	0.1	3.2	1.6
A	**P04**	0.5 ± 0.4	1.1	-0.2	-0.8	0.5	AP	0.3	1.0	0.7
	P08	2.9 ± 1.5	5.8	0.2	-0.9	0.4	AP	0.6	3.6	1.7
	P10	3.3 ± 1.8	5.2	0.0	-1.0	0.1	AP	0.2	3.7	0.5

Note: R – retroverted, N – normal flexion, A – anteverted uterus; Dir. – predominant direction of displacement based on the mean displacement vector coordinates; AP – antero-posterior direction, SI – superior-inferior direction; SD – standard deviation

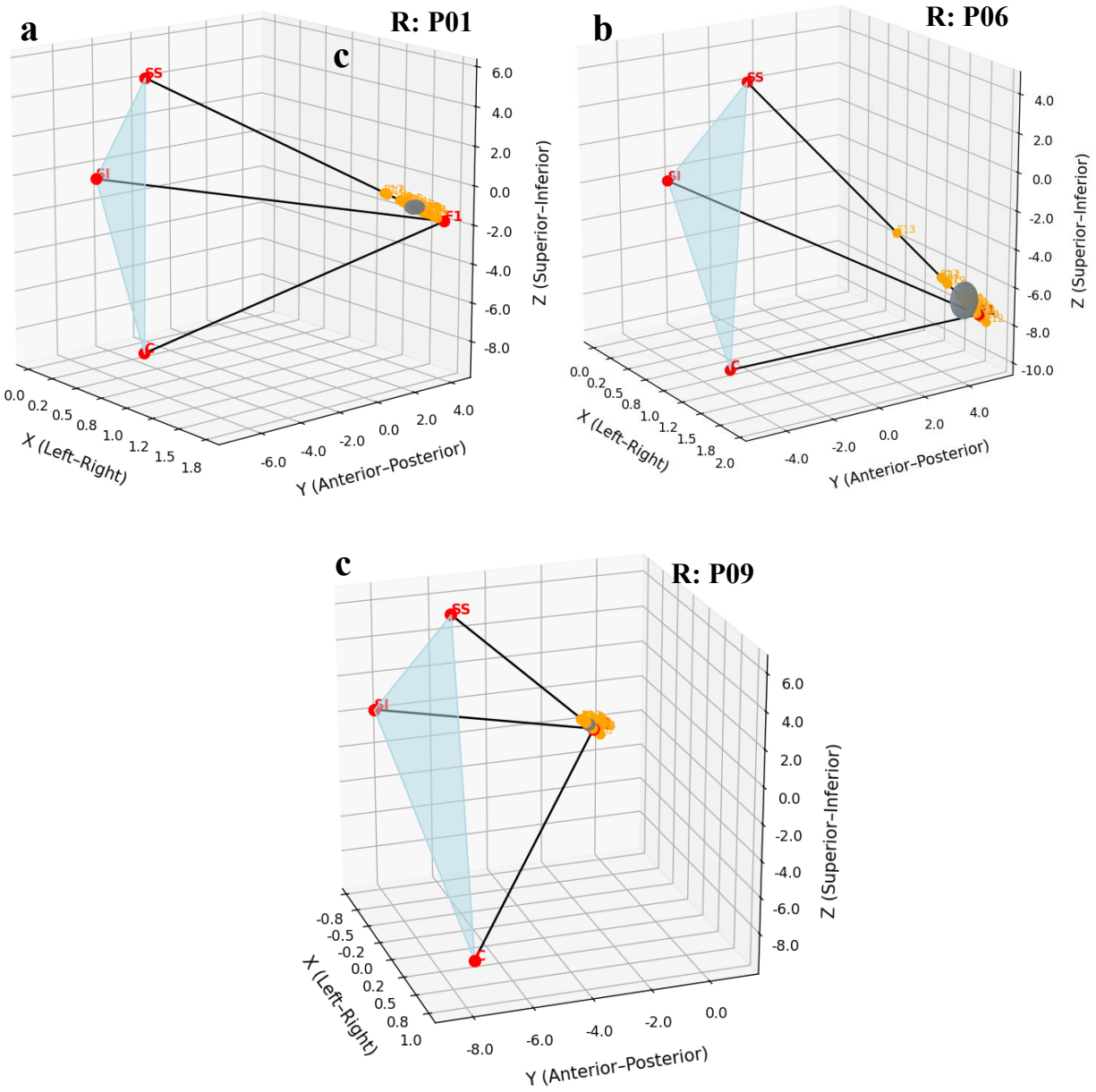

Figure 3.2: Three-dimensional plots depicting the anatomical geometry for the first fraction represented by the pyramidal structure (blue triangle, black lines), the points (orange) corresponding to the apexes derived from each fraction and the ellipsoid resulting from the displacement SDs in each spatial direction – retroverted uterus: (a) P01, (b) P06, (c) P09

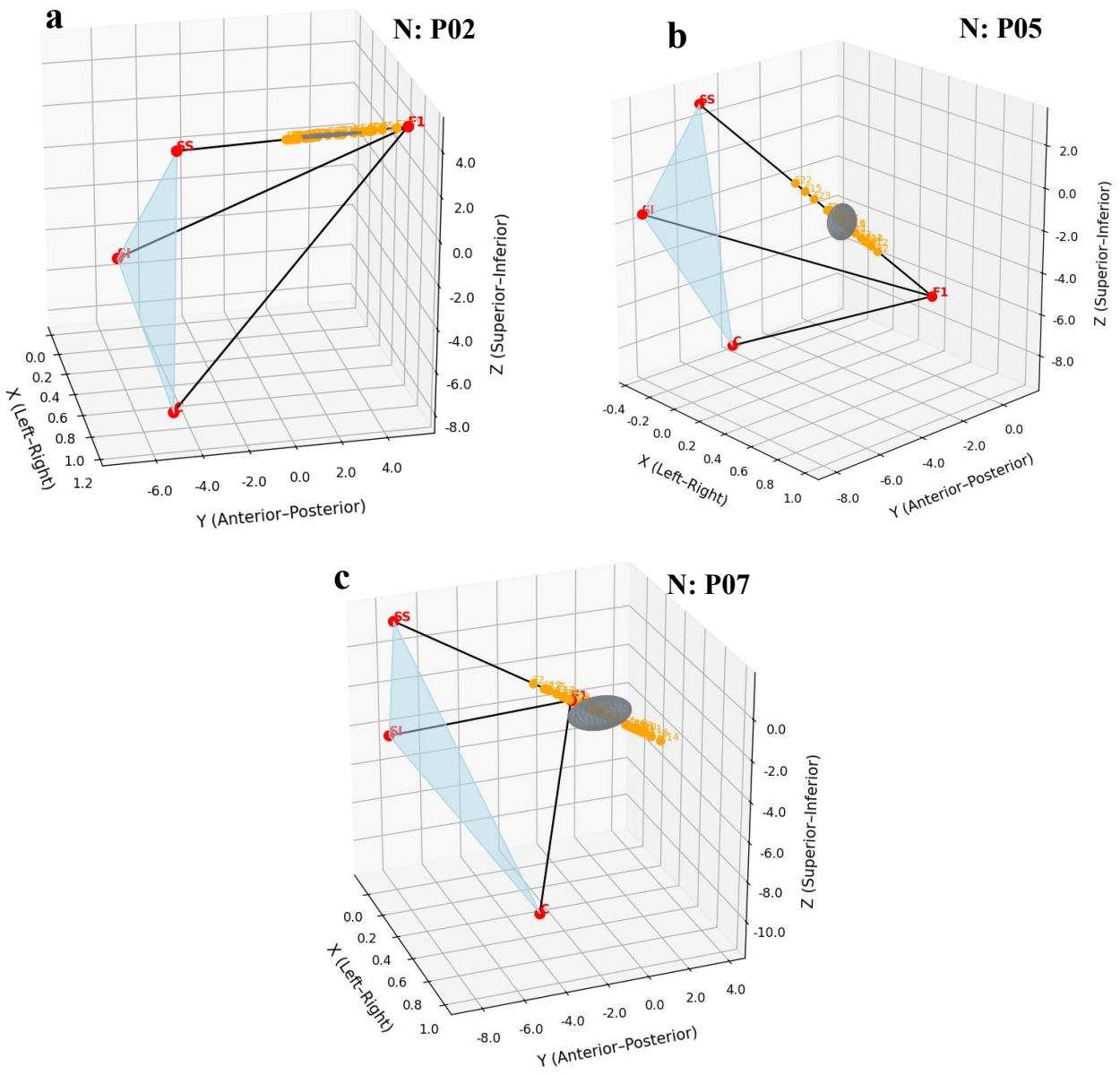

Figure 3.3: Uterus displacement visual representation in case of normal uterus: (a) P02, (b) P05, (c) P07

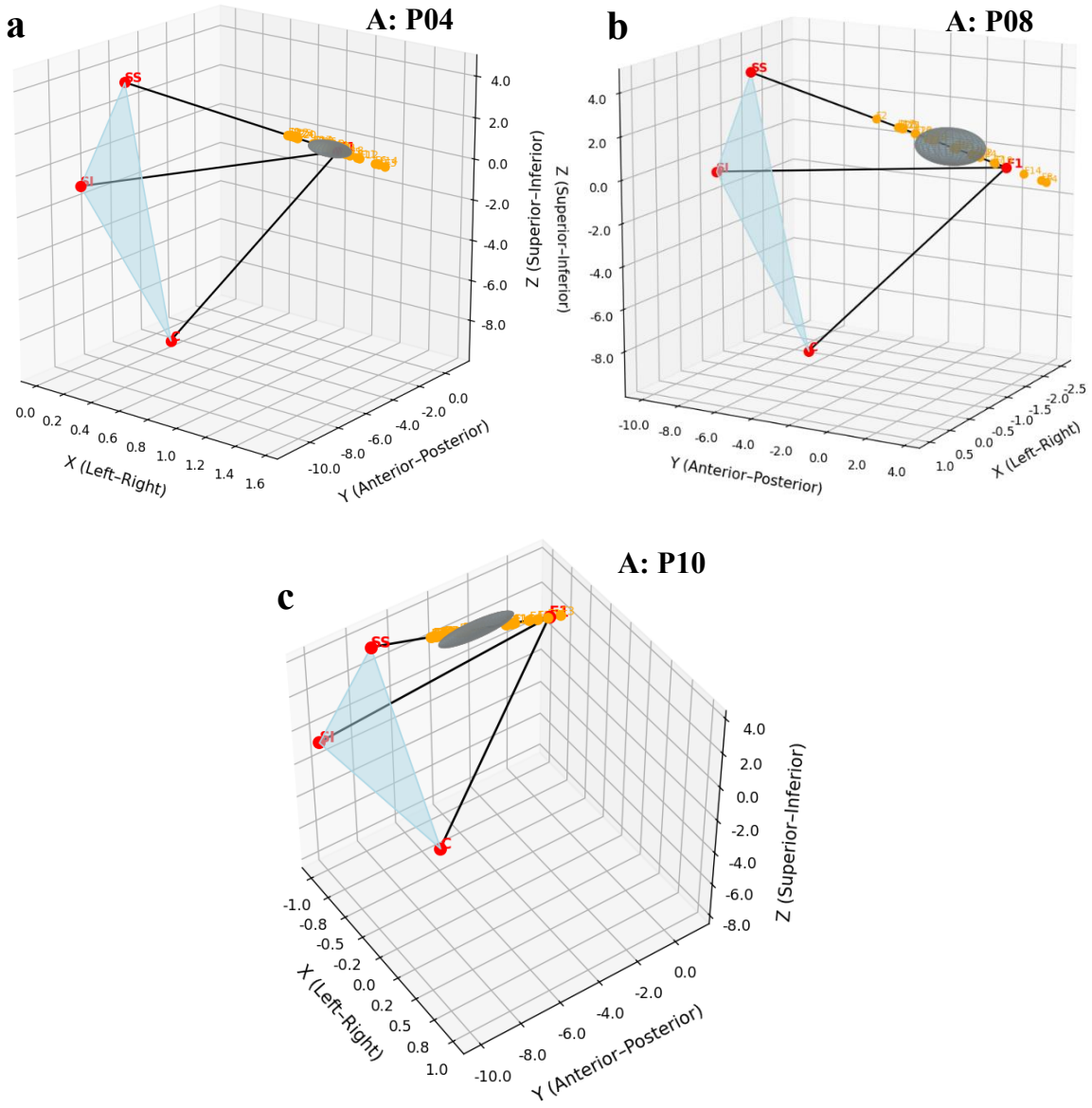

Figure 3.4: Uterus displacement visual representation in case of anteverted uterus: (a) P04, (b) P08, (c) P10

The results that evaluate the influence of bladder volume variation on the uterus spatial and directional motion are reported in Table 3.3. Weak correlations ($|r| \leq 3$) and non-significant p-values appear to describe the bladder volume influence on retroverted uteri, as described in Figure 3.5. These values confirm the unrelated anatomical relationship between this inherent posterior uterus position and the bladder dynamics in the anterior direction. Normal uteri display an overall strong response to changes

in bladder volume that seem to cause anterior-superior movement, (Δy: r = 0.8, p < 0.01, Δz: r = -0.8, p < 0.01), observation evidenced in Figure 3.6.

Table 3.3: Statistical analysis between the change in bladder volume ΔVB and the directional (Δx, Δy, Δz) and total uterus displacement (Δd) from the first fraction anatomical geometry, grouped by uterus flexion characteristics

Uterus	***ID***	**Δx**		**Δy**		**Δz**		**Δd**		***Mean ± SD***
		r	***p***	***r***	***p***	***r***	***p***	***r***	***p***	ΔV_B
	P01	0.2	0.275	0.2	0.275	-0.2	0.275	-0.2	0.275	0.5 ± 1.0
R	**P06**	0.3	0.146	0.3	0.146	-0.3	0.146	-0.3	0.238	-0.5 ± 0.3
	P09	-0.3	0.136	0.3	0.136	-0.3	0.136	-0.3	0.136	-0.7 ± 0.1
	P02	-0.8	< 0.01	0.8	< 0.01	-0.8	< 0.01	-0.8	< 0.01	-0.5 ± 0.3
N	**P05**	0.8	< 0.01	0.8	< 0.01	-0.8	< 0.01	-0.8	< 0.01	-0.4 ± 0.4
	P07	0.8	< 0.01	0.8	< 0.01	-0.8	< 0.01	0.7	< 0.01	0.1 ± 0.6
	P04	0.6	0.002	0.6	0.002	-0.6	0.002	0.1	0.625	-0.1 ± 0.9
A	**P08**	-0.7	< 0.01	0.7	< 0.01	-0.7	< 0.01	-0.5	0.007	-0.6 ± 0.3
	P10	0.8	< 0.01	0.8	< 0.01	-0.8	< 0.01	-0.9	p < 0.01	-0.6 ± 0.3

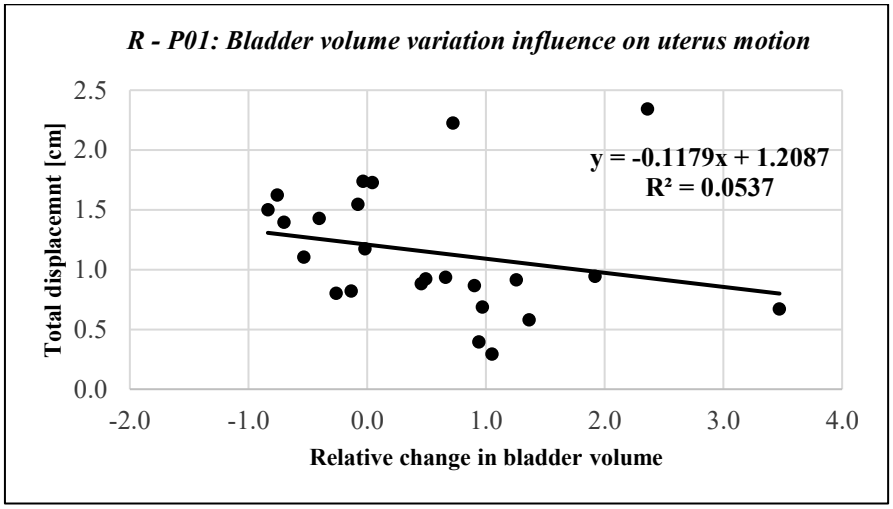

Figure 3.5 - Impact of bladder volume fluctuations on a retroverted uterus displacement (P01)

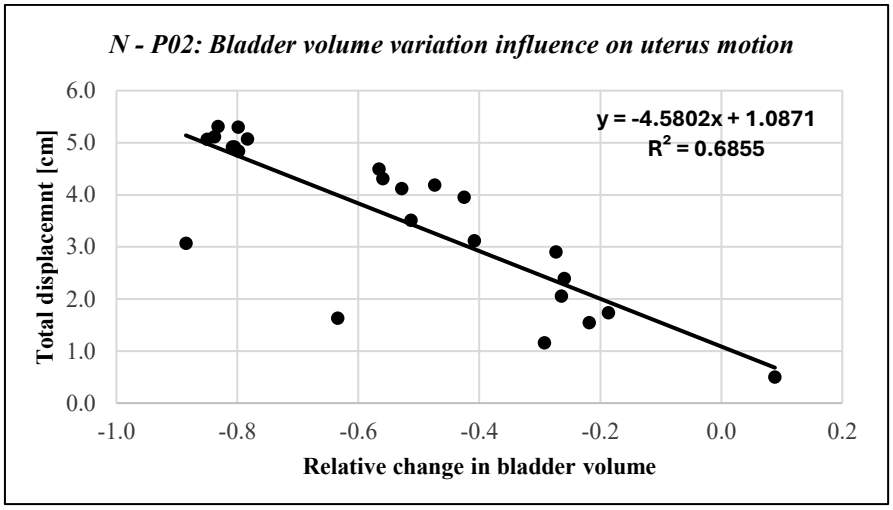

Figure 3.6 - Impact of bladder volume fluctuations on a normal uterus displacement (P02)

Likewise, anteverted uteri is greatly liable to display important displacement generated by bladder volume variations ($r = \pm 0.5 – 0.8$, $p < 0.01$), an idea visually supported by Figure 3.7. Total displacement does not significantly correlate with bladder changes in the case of P04, unlike the directional data, a situation that emphasize the importance of evaluating this parameter on each axis as constrained and balanced motion might be overlooked.

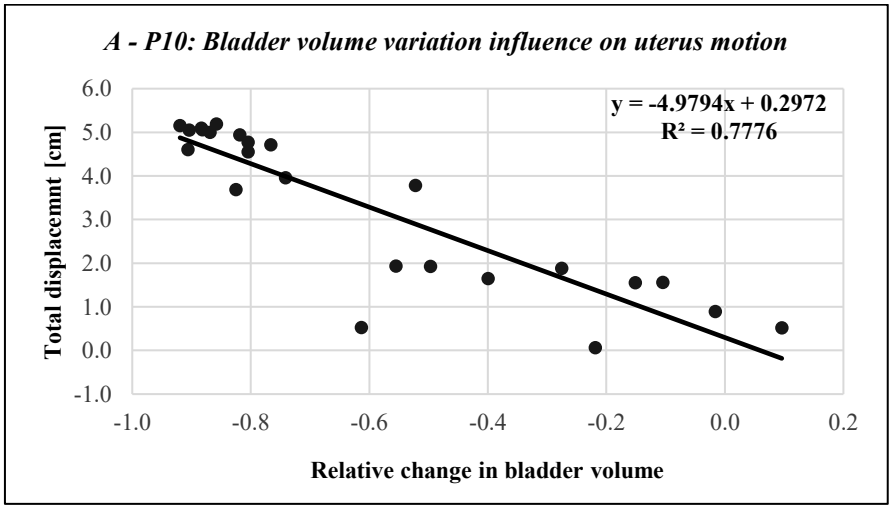

Figure 3.7 - Impact of bladder volume fluctuations on an anteverted uterus displacement (P10)

3.3. Uterus angle variation in superior-inferior direction

The statistical data evaluating the uterine motion by individually investigating the influence of bladder volume variation (ΔV_B) and the uterine angle modification ($\Delta\alpha$) with respect to the sacral promontory to confirm the superior-inferior direction displacements – see Figure 2.3 – is noted in Table 3.4. It was observed a meaningful variability between subjects, regarding both the direction and strength of correlation, as observed in Table 3.4.

Table 3.4: Correlation coefficients (r) and p-values analysis of uterus angle deviation ($\Delta\alpha$) in response to bladder volume variation

Uterus	***ID***	***r***	***p***	***Mean ± SD***
				$\Delta\alpha$
R	**P01**	0.2	0.303	0.9 ± 0.5
	P06	0.6	< 0.01	-0.2 ± 2.5
	P09	0.2	0.335	0.2 ± 0.2
N	**P02**	-0.8	< 0.01	0.1 ± 0.2
	P05	-0.4	0.090	0.1 ± 0.3
	P07	-0.8	< 0.01	0.1 ± 0.2
A	**P04**	-0.2	0.378	-0.1 ± 0.1
	P08	-0.6	< 0.01	0.2 ± 0.3
	P10	-0.5	0.011	-0.1 ± 0.1

The motion in the superior-inferior direction described by the retroverted uteri present inconsistent correlations with the changes in bladder volume, with significant values for P06 ($r = 0.6$, $p < 0.01$). This patient also stands out with a broader range of uterine angle modifications, suggesting high anatomical instability with a likely need of adaptative planning. Negative and moderate/strong correlations ($r = -0.4$ to -0.8) are specific for normal cases, suggesting a superiorly shifted uterus as a response to bladder filling, as depicted in Figure 3.8 validating the prior approaches that found important superior-inferior displacement (Δz: $r = -0.8$, $p < 0.01$). The moderate negative correlations and statistical relevance are also identified in the anteverted uteri, reiterating the previous statements of a concomitant antero-posterior and superior-inferior motions ($r = -0.6$ to -0.8, $p < 0.01$).

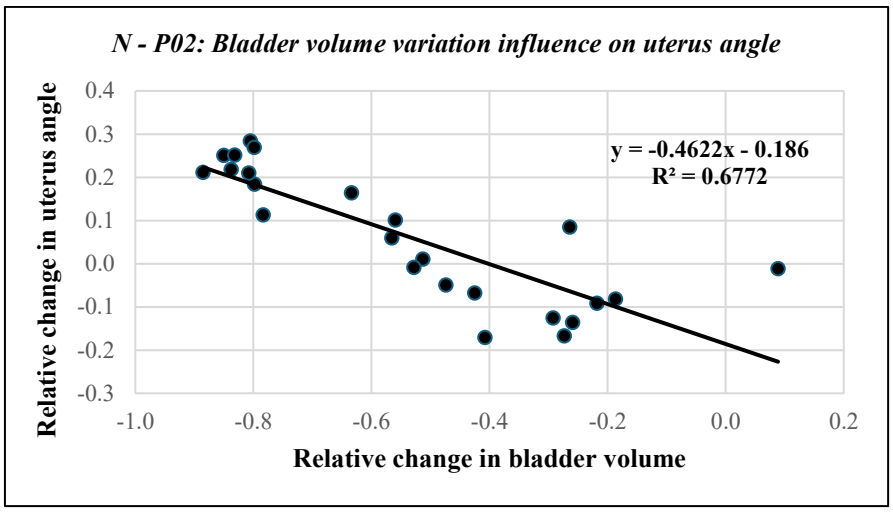

Figure 3.8: Representation of the strong negative correlation between the bladder volume variation and normal uterine angle modification during the treatment for P02

4. Discussions

4.1. Uterus displacement analysis

The retroverted uteri display an apparent stability that might allow for more controlled margins. Moreover, the normal uteri could benefit from ART capabilities as these cases exhibit significant inconstancy in terms of direction and extent of movement. All types of uteri demonstrated minimal values to describe left-right displacement that support the idea of reduced margins and increased predictability for treatment planning. These findings indicate that rigorously controlled bladder fillings protocols and individualized margins might improve the treatment precision for the patients that present normal and anteverted uteri. Thus, the previous 3D motion analysis is reiterated by the tendency of substantial anterior-posterior and superior-inferior movement of these uterus configurations, in contrast to the reduced movement described by the retroverted uteri. Ellipsoid modelling was crucial to visually represent motion envelopes in a spatial framework, presenting the magnitude, directionality and consistency among uterus types. Moreover, the noticeable variability in bladder volume could reflect inconsistent adherence to bladder protocols in opposition to better compliance or physiological consistency in bladder filling for the other patients, prompting it to be a slightly unpredictable parameter.

4.2. Uterus angle variation in superior-inferior direction

Despite the minimal displacement and correspondences illustrated by the previous method, the positive values, that would unexpectedly explain an angle growth as a result of bladder volume increase, suggest that the movement in the retroverted uteri cases is unpredictable and might be influenced by other anatomical and physiological aspects of every patient. It is further confirmed that the uterus flexion characteristics are a valuable factor in analysing its motion, notably in the superior-inferior direction, with possible additional considerations needed in margin definition of normal and anteverted cases. Moreover, as there is no clear evidence of a response pattern, it is suggested the need for patient-specific considerations, underscoring the importance of individualized and adapted protocols. Furthermore, this analysis also underscores the necessity of personalized and individualized monitoring strategies, especially of the bladder filling protocols as it is seemingly greatly influenced by patient particularities.

In comparison with the other referenced articles using this type of treatment machine, there are differences regarding the temporal aspect of the data acquisitions and the method of correlating the bladder filling and the uterine movement, without focusing on quantifying it. Moreover, this study individualizes by the analysis according to the uterus anatomical orientation. The 3D study of Kishigami *et al.* reached the conclusions that the daily interfractional variations were unpredictable and that the uterine displacement progressively increased over the course of treatment, with expended margins in all direction relative to conventional and other studies' values [59]. They also deduced that the 16th fraction is a suitable choice of treatment replanning, as the cervical volume decreased with 50%. The pre- and post-treatment MR images, in the DSC-based intrafractional assessment made by Nagao *et al.*, revealed that the bladder filling has the most impact on the superior-posterior direction, with patient-specific response for uterine displacement extent, being a confirmation of the current study [57]. In their analysis, by employing 5 imaging types at various time points, Li *et al.* reported an important intra- and inter-fractional cervix-uterus motion, predominantly in anterio-posterior and cranio-caudal directions, that correlates with fluctuations in bladder volume, further validating the conclusions of this thesis.

Among the leading drawbacks of this study are the limited number of included patients that restricts the possibility of reaching a generalized conclusion, the resolution and slice distances that occasionally hindered the perfect localisation of a certain point and the susceptibility of the observations and measurements to inter-observer variations. Moreover, the assumption that the bony reference points have the exact position over the course of treatment might induce some errors.

This research project could be completed and improved by concomitantly assessing the cervix motion, adding the rectum filling correlations and by employing 3D modelling programmes such as 3D Slicer or MeshLab in order to compute the interfractional displacement, a sample being presented in Figure 3.10 [60 - 63].

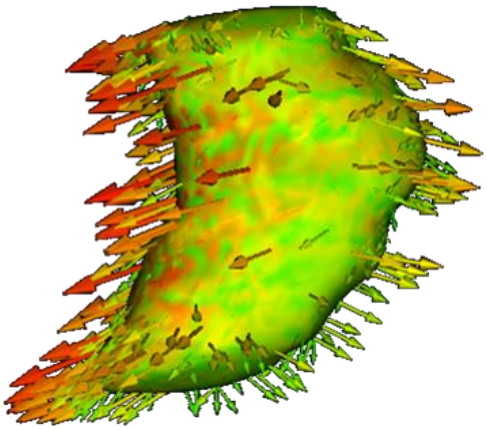

Figure 3.9: A sample of interfractional displacement vectors visual representation for two uterus contours obtained using ModelToModelDistance and ShapePopulationViewer modules from 3DSlicer software

Conclusions

Taking everything into consideration, the findings of this research study added a comprehensive spatial and directional analysis of the daily uterine motion in correlation with the bladder volume variation for cervix cancer patients treated with Unity® MR-Linac system, further enhanced by adding the classification of these results according to the uterus configuration – retroverted, normal or anteverted.

By integrating DICOM coordinates with geometrical and statistical evaluation, in the case of 9 patients, the change in uterus position was characterized throughout 25 fraction of radiotherapy treatment in relation to bladder volume, based on the first fraction anatomical characteristics. In terms of directional preference, the results demonstrated that, while the anteverted and normal uteri displayed statistically significant correlations and important movement chiefly occurred in anterior-posterior and superior-inferior planes, the retroverted uteri had an insignificant and unpredictable response to bladder filling.

Fundamentally, these aspects have particular clinical value when presented in the context of ART as precise and real-time quantification of inter-fraction variations of anatomical structures are essential, alongside motion margin customization. This work emphasizes the need for bladder filling protocols and facilitates the identification of cases that may require selective adaptation workflows because of unforeseen displacements, such as those with normal or anteverted uteri and important bladder variability.

Bibliography

[1] F. Bray *et al.*, "Global cancer statistics 2022: GLOBOCAN estimates of incidence and mortality worldwide for 36 cancers in 185 countries," *CA Cancer J Clin*, vol. 74, no. 3, pp. 229–263, May 2024, doi: 10.3322/caac.21834.

[2] J. Ferlay *et al.*, "Global Cancer Observatory: Cancer Today." Accessed: Dec. 04, 2024. [Online]. Available: https://gco.iarc.who.int/today/en

[3] World Health Organization, *Global strategy to accelerate the elimination of cervical cancer as a public health problem*. World Health Organization, 2020.

[4] eClinicalMedicine, "Global strategy to eliminate cervical cancer as a public health problem: are we on track?," *EClinicalMedicine*, vol. 55, p. 101842, Jan. 2023, doi: 10.1016/j.eclinm.2023.101842.

[5] D. Cibula *et al.*, "The European Society of Gynaecological Oncology/European Society for Radiotherapy and Oncology/European Society of Pathology Guidelines for the Management of Patients with Cervical Cancer," *Virchows Archiv*, vol. 472, no. 6, pp. 919–936, Jun. 2018, doi: 10.1007/s00428-018-2362-9.

[6] R. Jadon *et al.*, "A Systematic Review of Organ Motion and Image-guided Strategies in External Beam Radiotherapy for Cervical Cancer," *Clin Oncol*, vol. 26, no. 4, pp. 185–196, Apr. 2014, doi: 10.1016/j.clon.2013.11.031.

[7] M. A. Ameer, S. E. Fagan, J. N. Sosa-Stanley, and D. C. Peterson, "Anatomy, Abdomen and Pelvis: Uterus.," in *StatPearls [Internet]*, Treasure Island (FL): StatPearls Publishing;, 2022. Accessed: Dec. 04, 2024. [Online]. Available: https://www.ncbi.nlm.nih.gov/books/NBK470297/

[8] M. K. Roach and R. F. Andreotti, "The Normal Female Pelvis," *Clin Obstet Gynecol*, vol. 60, no. 1, pp. 3–10, Mar. 2017, doi: 10.1097/GRF.0000000000000259.

[9] Walter. Prendiville and R. . Sankaranarayanan, "Anatomy of the uterine cervix and the transformation zone," in *Colposcopy and Treatment of Cervical Precancer*, Lyon (FR): International Agency for Research on Cancer, 2017, ch. 2, pp. 13–21. Accessed: Dec. 04, 2024. [Online]. Available: https://www.ncbi.nlm.nih.gov/books/NBK568392/

[10] National Cancer Institute, "What is Cervical Cancer?" Accessed: Dec. 04, 2024. [Online]. Available: https://www.cancer.gov/types/cervical

[11] Jain MA and Limaiem F., "Cervical Squamous Cell Carcinoma," in *StatPearls [Internet]*, Treasure Island (FL): StatPearls Publishing, 2023. Accessed: Dec. 04, 2024. [Online]. Available: https://www.ncbi.nlm.nih.gov/books/NBK559075/

[12] C. A. Burmeister *et al.*, "Cervical cancer therapies: Current challenges and future perspectives," *Tumour Virus Res*, vol. 13, p. 200238, Jun. 2022, doi: 10.1016/j.tvr.2022.200238.

[13] National Cancer Institute, "Cervical Cancer Screening," May 2024. [Online]. Available: https://www.cancer.gov/types/cervical/screening

[14] National Cancer Institute, "Cervical Cancer Diagnosis." [Online]. Available: https://www.cancer.gov/types/cervical/diagnosis

[15] N. Bhatla, S. Singhal, E. Dhamija, S. Mathur, J. Natarajan, and A. Maheshwari, "Implications of the revised cervical cancer FIGO staging system," *Indian Journal of Medical Research*, vol. 154, no. 2, p. 273, 2021, doi: 10.4103/ijmr.IJMR_4225_20.

[16] N. Bhatla *et al.*, "Revised FIGO staging for carcinoma of the cervix uteri," *International Journal of Gynecology & Obstetrics*, vol. 145, no. 1, pp. 129–135, Apr. 2019, doi: 10.1002/ijgo.12749.

[17] M. Y. Salib *et al.*, "2018 FIGO Staging Classification for Cervical Cancer: Added Benefits of Imaging," *RadioGraphics*, vol. 40, no. 6, pp. 1807–1822, Oct. 2020, doi: 10.1148/rg.2020200013.

[18] J. C. A. Dimopoulos *et al.*, "Recommendations from Gynaecological (GYN) GEC-ESTRO Working Group (IV): Basic principles and parameters for MR imaging within the frame of image based adaptive cervix cancer brachytherapy," *Radiotherapy and Oncology*, vol. 103, no. 1, pp. 113–122, Apr. 2012, doi: 10.1016/j.radonc.2011.12.024.

[19] M. F. M. L. T. Tan MBBS *et al.*, "Image-guided Adaptive Radiotherapy in Cervical Cancer," *Semin Radiat Oncol*, vol. 29, no. 3, pp. 284–298, Jul. 2019, doi: 10.1016/j.semradonc.2019.02.010.

[20] National Cancer Insitute, "Cervical Cancer Treatment by Stage." [Online]. Available: https://www.cancer.gov/types/cervical/treatment/by-stage

[21] K. Tanderup, D. Georg, R. Pötter, C. Kirisits, C. Grau, and J. C. Lindegaard, "Adaptive Management of Cervical Cancer Radiotherapy," *Semin Radiat Oncol*, vol. 20, no. 2, pp. 121–129, Apr. 2010, doi: 10.1016/j.semradonc.2009.11.006.

[22] C. A. Johnson, D. James, A. Marzan, and M. Armaos, "Cervical Cancer: An Overview of Pathophysiology and Management," *Semin Oncol Nurs*, vol. 35, no. 2, pp. 166–174, Apr. 2019, doi: 10.1016/j.soncn.2019.02.003.

[23] S. Ghosh *et al.*, "Clinical Implementation of 'Plan of the Day' Strategy in Definitive Radiation Therapy of Cervical Cancer: Online Adaptation to Address the Challenge of Organ Filling Reproducibility," *International Journal of Radiation Oncology*Biology*Physics*, vol. 118, no. 3, pp. 605–615, Mar. 2024, doi: 10.1016/j.ijrobp.2023.09.045.

[24] J. Bertholet *et al.*, "Real-time intrafraction motion monitoring in external beam radiotherapy," *Phys Med Biol*, vol. 64, no. 15, p. 15TR01, Aug. 2019, doi: 10.1088/1361-6560/ab2ba8.

[25] I. M. White *et al.*, "Realizing the potential of magnetic resonance image guided radiotherapy in gynaecological and rectal cancer," *Br J Radiol*, p. 20180670, May 2019, doi: 10.1259/bjr.20180670.

[26] F. Slevin, M. Beasley, R. Speight, J. Lilley, L. Murray, and A. Henry, "Overview of patient preparation strategies to manage internal organ motion during radiotherapy in the pelvis," *J Radiother Pract*, vol. 19, no. 2, pp. 182–189, Jun. 2020, doi: 10.1017/S1460396919000530.

[27] M. Ingle and S. Lalondrelle, "Current Status of Anatomical Magnetic Resonance Imaging in Brachytherapy and External Beam Radiotherapy Planning and Delivery," *Clin Oncol*, vol. 32, no. 12, pp. 817–827, Dec. 2020, doi: 10.1016/j.clon.2020.10.009.

[28] L. van de Bunt, I. M. Jürgenliemk-Schulz, G. A. P. de Kort, J. M. Roesink, R. J. H. A. Tersteeg, and U. A. van der Heide, "Motion and deformation of the target volumes during IMRT for cervical cancer: What margins do we need?," *Radiotherapy and Oncology*, vol. 88, no. 2, pp. 233–240, Aug. 2008, doi: 10.1016/j.radonc.2007.12.017.

[29] A. Taylor and M. E. B. Powell, "An assessment of interfractional uterine and cervical motion: Implications for radiotherapy target volume definition in gynaecological cancer," *Radiotherapy and Oncology*, vol. 88, no. 2, pp. 250–257, Aug. 2008, doi: 10.1016/j.radonc.2008.04.016.

[30] I. Ríos, I. Vásquez, E. Cuervo, Ó. Garzón, and J. Burbano, "Problems and solutions in IGRT for cervical cancer," *Reports of Practical Oncology & Radiotherapy*, vol. 23, no. 6, pp. 517–527, Nov. 2018, doi: 10.1016/j.rpor.2018.05.002.

[31] A. Naik, O. P. Gurjar, K. L. Gupta, K. Singh, P. Nag, and V. Bhandari, "Comparison of dosimetric parameters and acute toxicity of intensity-modulated and three-dimensional radiotherapy in patients with cervix carcinoma: A randomized prospective study," *Cancer/Radiothérapie*, vol. 20, no. 5, pp. 370–376, Jul. 2016, doi: 10.1016/j.canrad.2016.05.011.

[32] L. Portelance, K. S. C. Chao, P. W. Grigsby, H. Bennet, and D. Low, "Intensity-modulated radiation therapy (IMRT) reduces small bowel, rectum, and bladder doses in patients with cervical cancer receiving pelvic and para-aortic irradiation," *International Journal of Radiation Oncology*Biology*Physics*, vol. 51, no. 1, pp. 261–266, Sep. 2001, doi: 10.1016/S0360-3016(01)01664-9.

[33] H. Kim, S. Beriwal, M. S. Huq, N. Kannan, G. Shukla, and C. Houser, "Evaluation of Set-up Uncertainties with Daily Kilovoltage Image Guidance in External Beam Radiation Therapy for Gynaecological Cancers," *Clin Oncol*, vol. 24, no. 2, pp. e39–e45, Mar. 2012, doi: 10.1016/j.clon.2011.09.007.

[34] E. M. Kerkhof, R. W. van der Put, B. W. Raaymakers, U. A. van der Heide, I. M. Jürgenliemk-Schulz, and J. J. W. Lagendijk, "Intrafraction motion in patients with cervical cancer: The benefit of soft tissue registration using MRI," *Radiotherapy and Oncology*, vol. 93, no. 1, pp. 115–121, Oct. 2009, doi: 10.1016/j.radonc.2009.07.010.

[35] S. Bipat, A. S. Glas, J. van der Velden, A. H. Zwinderman, P. M. M. Bossuyt, and J. Stoker, "Computed tomography and magnetic resonance imaging in staging of uterine cervical carcinoma: a systematic review," *Gynecol Oncol*, vol. 91, no. 1, pp. 59–66, Oct. 2003, doi: 10.1016/S0090-8258(03)00409-8.

[36] D. G. Mitchell *et al.*, "Early Invasive Cervical Cancer: Tumor Delineation by Magnetic Resonance Imaging, Computed Tomography, and Clinical Examination, Verified by Pathologic Results, in the ACRIN 6651/GOG 183 Intergroup Study," *Journal of Clinical Oncology*, vol. 24, no. 36, pp. 5687–5694, Dec. 2006, doi: 10.1200/JCO.2006.07.4799.

[37] E. M. Kerkhof, B. W. Raaymakers, U. A. van der Heide, L. van de Bunt, I. M. Jürgenliemk-Schulz, and J. J. W. Lagendijk, "Online MRI guidance for healthy tissue sparing in patients with cervical cancer: An IMRT planning study," *Radiotherapy and Oncology*, vol. 88, no. 2, pp. 241–249, Aug. 2008, doi: 10.1016/j.radonc.2008.04.009.

[38] C. Balleyguier *et al.*, "Staging of uterine cervical cancer with MRI: guidelines of the European Society of Urogenital Radiology," *Eur Radiol*, vol. 21, no. 5, pp. 1102–1110, May 2011, doi: 10.1007/s00330-010-1998-x.

[39] E. Vincens *et al.*, "Accuracy of magnetic resonance imaging in predicting residual disease in patients treated for stage IB2/II cervical carcinoma with chemoradiation therapy," *Cancer*, vol. 113, no. 8, pp. 2158–2165, Oct. 2008, doi: 10.1002/cncr.23817.

[40] A. Hunt, V. N. Hansen, U. Oelfke, S. Nill, and S. Hafeez, "Adaptive Radiotherapy Enabled by MRI Guidance," *Clin Oncol*, vol. 30, no. 11, pp. 711–719, Nov. 2018, doi: 10.1016/j.clon.2018.08.001.

[41] B. Anghel, C. Serboiu, A. Marinescu, I.-A. Taciuc, F. Bobirca, and A. D. Stanescu, "Recent Advances and Adaptive Strategies in Image Guidance for Cervical Cancer Radiotherapy," *Medicina (B Aires)*, vol. 59, no. 10, p. 1735, Sep. 2023, doi: 10.3390/medicina59101735.

[42] C. E. Shelley, L. H. Barraclough, C. L. Nelder, S. J. Otter, and A. J. Stewart, "Adaptive Radiotherapy in the Management of Cervical Cancer: Review of Strategies and Clinical Implementation," *Clin Oncol*, vol. 33, no. 9, pp. 579–590, Sep. 2021, doi: 10.1016/j.clon.2021.06.007.

[43] W. A. Hall *et al.*, "Magnetic resonance linear accelerator technology and adaptive radiation therapy: An overview for clinicians," *CA Cancer J Clin*, vol. 72, no. 1, pp. 34–56, Jan. 2022, doi: 10.3322/caac.21707.

[44] L. Portelance *et al.*, "Online Magnetic Resonance-Guided Radiotherapy (oMRgRT) for Gynecological Cancers," *Front Oncol*, vol. 11, Aug. 2021, doi: 10.3389/fonc.2021.628131.

[45] S. Corradini *et al.*, "MR-guidance in clinical reality: current treatment challenges and future perspectives," *Radiation Oncology*, vol. 14, no. 1, p. 92, Dec. 2019, doi: 10.1186/s13014-019-1308-y.

[46] Elekta, "Elekta Unity MR-Linac - MR/RT. Radiotherapy", Accessed: Dec. 06, 2024. [Online]. Available: https://www.elekta.com/products/radiation-therapy/unity/

[47] J. J. W. Lagendijk *et al.*, "MRI/linac integration," *Radiotherapy and Oncology*, vol. 86, no. 1, pp. 25–29, Jan. 2008, doi: 10.1016/j.radonc.2007.10.034.

[48] J. J. W. Lagendijk, B. W. Raaymakers, and M. van Vulpen, "The Magnetic Resonance Imaging–Linac System," *Semin Radiat Oncol*, vol. 24, no. 3, pp. 207–209, Jul. 2014, doi: 10.1016/j.semradonc.2014.02.009.

[49] J. J. W. Lagendijk, B. W. Raaymakers, M. P. W. Intven, and J. R. N. van der Voort van Zyp, "ESTRO Breur lecture 2022: Real-time MRI-guided radiotherapy: The next generation standard?," *Radiotherapy and Oncology*, vol. 176, pp. 244–248, Nov. 2022, doi: 10.1016/j.radonc.2022.08.021.

[50] D. A. Roberts *et al.*, "Machine QA for the Elekta Unity system: A Report from the Elekta MR-linac consortium," *Med Phys*, vol. 48, no. 5, May 2021, doi: 10.1002/mp.14764.

[51] J. Zhong *et al.*, "MRI-guided Pelvic Radiation Therapy: A Primer for Radiologists," *RadioGraphics*, vol. 43, no. 11, Nov. 2023, doi: 10.1148/rg.230052.

[52] J. de Leon, T. Twentyman, M. Carr, M. Jameson, and V. Batumalai, "Optimising the MR-Linac as a standard treatment modality," *J Med Radiat Sci*, vol. 70, no. 4, pp. 491–497, Dec. 2023, doi: 10.1002/jmrs.712.

[53] D. Winkel *et al.*, "Individual lymph nodes: 'See it and Zap it,'" *Clin Transl Radiat Oncol*, vol. 18, pp. 46–53, Sep. 2019, doi: 10.1016/j.ctro.2019.03.004.

[54] S. Ding *et al.*, "MRI guided online adaptive radiotherapy and the dosimetric impact of inter- and intrafractional motion in patients with cervical cancer," *Clin Transl Radiat Oncol*, vol. 50, p. 100881, Jan. 2025, doi: 10.1016/j.ctro.2024.100881.

[55] J. Ng *et al.*, "MRI-LINAC: A transformative technology in radiation oncology," *Front Oncol*, vol. 13, Jan. 2023, doi: 10.3389/fonc.2023.1117874.

[56] P. Chan *et al.*, "Inter- and Intrafractional Tumor and Organ Movement in Patients With Cervical Cancer Undergoing Radiotherapy: A Cinematic-MRI Point-of-Interest Study," *International Journal of Radiation Oncology*Biology*Physics*, vol. 70, no. 5, pp. 1507–1515, Apr. 2008, doi: 10.1016/j.ijrobp.2007.08.055.

[57] A. Nagao *et al.*, "Assessment of intrafractional motion of the cervix–uterus by MR-guided radiotherapy system," *J Radiat Res*, vol. 64, no. 6, pp. 967–972, Nov. 2023, doi: 10.1093/jrr/rrad072.

[58] X. Li *et al.*, "Online MR evaluation of inter- and intra-fraction uterus motions and bladder volume changes during cervical cancer external beam radiotherapy," *Radiation Oncology*, vol. 16, no. 1, p. 179, Dec. 2021, doi: 10.1186/s13014-021-01907-1.

[59] Y. Kishigami, M. Nakamura, M. Nakao, H. Okamoto, A. Takahashi, and H. Igaki, "Three-dimensional assessment of interfractional cervical and uterine motions using daily magnetic resonance images to determine margins and timing of replanning," *J Appl Clin Med Phys*, vol. 24, no. 10, Oct. 2023, doi: 10.1002/acm2.14073.

[60] "3D Slicer image computing platform." Accessed: Jun. 23, 2025. [Online]. Available: https://www.slicer.org/

[61] R. Kikinis, S. D. Pieper, and K. G. Vosburgh, "3D Slicer: A Platform for Subject-Specific Image Analysis, Visualization, and Clinical Support," in *Intraoperative Imaging and Image-Guided Therapy*, New York, NY: Springer New York, 2014, pp. 277–289. doi: 10.1007/978-1-4614-7657-3_19.

[62] A. Fedorov *et al.*, "3D Slicer as an image computing platform for the Quantitative Imaging Network," *Magn Reson Imaging*, vol. 30, no. 9, pp. 1323–1341, Nov. 2012, doi: 10.1016/j.mri.2012.05.001.

[63] P. Cignoni, M. Callieri, M. Corsini, M. Dellepiane, F. Ganovelli, and G. Ranzuglia, "MeshLab: an Open-Source Mesh Processing Tool," Pisa, Italy, 2008.